# Fingerprinting fluid source in calcite veins: combining LA-ICP-MS U-Pb calcite dating with trace elements and clumped isotope palaeothermometry

J. M. MacDonald[1], J. VanderWal[2], N. M. W. Roberts[3], I. Z. Winkelstern[4], J. W. Faithfull[5], A. J. Boyce[6]

[1]School of Geographical and Earth Sciences, University of Glasgow, Glasgow G12 8QQ, UK
[2] Mineral Deposits Laboratory, Department of Earth Sciences, Carleton University, Ottawa ON K1S 5B6
[3]Geochronology and Tracers Facility, British Geological Survey, Environmental Science Centre, Nottingham, NG12 5GG, UK
[4]Department of Geology, Grand Valley State University, 145 Padnos Hall of Science, 1 Campus Drive, Allendale, MI 49401, USA
[5]The Hunterian, University of Glasgow, Glasgow G12 8QQ, UK
[6]NERC Isotope Community Support Facility, Scottish Universities Environmental Research Centre, Rankine Avenue, Scottish Enterprise Technology Park, East Kilbride G75 0QF, UK

ABSTRACT

Application of geochemical proxies to vein minerals - particularly calcite - can fingerprint the source of fluids controlling various important geological processes from seismicity to geothermal systems. Determining fluid source, e.g. meteoric, marine, magmatic or metamorphic waters, can be challenging when using only trace elements and stable isotopes as different fluids can have overlapping geochemical characteristics, such as $\delta^{18}O$. In this contribution we show that by combining the recently developed LA-ICP-MS U-Pb calcite geochronometer with stable isotopes (including clumped isotope palaeothermometry) and trace element analysis, the fluid source of veins can be more readily determined. Calcite veins hosted in the Devonian Montrose Volcanic Formation at Lunan Bay in the Midland Valley Terrane of Central Scotland were used as a case study. δD values of fluid inclusions in the calcite, and parent fluid $\delta^{18}O$ values reconstructed from clumped isotope palaeothermometry, gave values which could represent a range of fluid sources: metamorphic or magmatic fluids, or surface waters which had undergone much fluid-rock interaction. Trace elements showed no distinctive patterns and shed no further light on fluid source. LA-ICP-MS U-Pb dating determined the vein calcite precipitation age – 318±30 Ma – which rule out metamorphic or magmatic fluid sources as no metamorphic or magmatic activity was occurring in the area at this time. The vein fluid source was therefore a surface water (meteoric based on paleogeographic reconstruction) which had undergone significant water-rock interaction. This study highlights the importance of combining the recently developed LA-ICP-MS U-Pb calcite geochronometer with stable isotopes and trace elements to help determine fluid sources of veins, and indeed any geological feature where calcite precipitated from a fluid that may have resided in the crust for a period of time (e.g. fault precipitates or cements).

Keywords: LA-ICP-MS U-Pb calcite geochronology; clumped isotopes; fluid δD and $\delta^{18}O$; calcite veins; trace elements.

## INTRODUCTION

Fingerprinting the source of fluids flowing through fractures in the crust has importance in a range of geological applications, including: 1) understanding the origin, and predicting sustainability, of geothermal systems (e.g. Simmons and Christenson 1994; Menzies et al. 2014; Lu et al. 2017; Lu et al. 2018); 2) determining the origin and concentration of economic mineral deposits (e.g. Barker and Cox 2011); and 3) reconstructing fluid flow pathways responsible for seismicity (e.g. Uysal et al. 2011; Sturrock et al. 2017). Evidence of fluid flow through fractures is recorded by the presence of veins and application of geochemical proxies to vein minerals - particularly calcite - can enable reconstruction of fluid sources.

If stable isotope signatures of vein-forming minerals can be reconstructed, then this has the potential to enable fluid source identification. The hydrogen isotopic signature (δD) of vein-forming fluids can be measured by decrepitation if there is a high enough volume of fluid inclusions within the vein-filling calcite (Gleeson et al. 2008). Fluid $\delta^{18}O$ can be calculated by determining the calcite $\delta^{18}O$ and the temperature of precipitation (e.g. Epstein et al. 1951). Precipitation temperature of calcite veins can be reconstructed from fluid inclusion microthermometry (e.g. Barker and Goldstein 1990; Maskenskaya et al. 2014) or the more recently-developed clumped isotope palaeothermometer. Clumped isotope palaeothermometry utilises the temperature dependence of different isotopologues of $CO_2$, particularly the mass 47 $^{13}C$-$^{18}O$-$^{16}O$ isotopologue (e.g. Schauble et al. 2006; Eiler 2007). Calcite vein precipitation temperatures have been reconstructed using clumped isotopes in geothermal/hydrothermal systems (Lu et al. 2017; Lu et al. 2018; MacDonald et al. 2019), sedimentary basins (Mangenot et al. 2018a; Pagel et al. 2018) and fault systems (Bergman et al. 2013; Hodson et al. 2016).

Stable isotope analysis can therefore provide details of the vein-forming fluid source. Different fluids (e.g. magmatic, metamorphic, meteoric, seawater) have typical compositions in δD-$\delta^{18}O$ (V-SMOW) space (e.g. Craig 1961; Taylor 1974; Rollinson 1993; Sharp 2007; Hoefs 2015). However, these different fluids may have overlapping compositions, or their isotopic composition may have changed over time. For example, a water with δD of -50 ‰ and $\delta^{18}O$ of +8 ‰ could be a magmatic water or a metamorphic water (e.g. Hoefs 2015); equally though, it could be a meteoric water

which has undergone significant water-rock equilibration resulting in an enrichment of $\delta^{18}O$ (e.g. Menzies et al. 2014). Thus, fluid stable isotope signatures in themselves do not always provide a conclusive fingerprint of palaeofluid sources, especially in settings such as veins where there is scope for significant water-rock interaction, and where genetic context of the hydrothermal system may be equivocal.

Previous studies attempting to determine the origin of vein-forming fluids have often analysed trace element concentrations in addition to stable isotopes. Barker et al., (2006) suggested varying trace element concentrations (and stable isotope values) in anti-taxial veins could be caused by cycles of fluid influx, water-rock interaction, and/or crack-seal processes. Maskenskaya et al., (2014) found that trace element concentrations and distribution in veins did not correlate with stable isotope (C, O, Sr) values; fractionation patterns of rare earth elements (REEs) were observed but again these could not be correlated with any measured chemical, physical and isotopic variables and so did not help to determine fluid source or vein formation mechanisms. Kalliomäki et al. (2019) compared the trace element signatures of vein calcite and their host rock and showed in examples from the Hattu schist belt (Finland) that interaction between the vein-forming fluid and the host rock had strongly influenced the trace element signature of the resulting vein calcite. Similarly, Wagner et al. (2010) used REEs to show that veins from the Rhenish Massif (Germany) formed from advecting fluids which leached the wall rocks, which was reflected in vein mineral trace element signatures.

The geological history of an area provides crucial context for discussion of potential fluid sources. In a metamorphic terrane, clearly metamorphic fluids may be recorded. With veins, however, fluid circulation may come sometime after formation of the surrounding geology and so linking vein-forming fluids to host rocks is more complex. Establishing the age of precipitation of veins is therefore key here to understanding the geological context of vein formation, and thus the likely fluids involved. For example, if a vein with a calculated fluid $\delta^{18}O$ of +9 ‰ and $\delta D$ of -50 ‰ can be dated to within error of formation of nearby basalts, then a contribution of magmatic fluids to vein precipitation cannot be discounted. The recent development of calcite U-Pb dating via Laser Ablation Inductively Coupled Mass Spectrometry (LA-ICP-MS) has enabled precise, accurate and rapid dating of calcite (e.g. Li et al. 2014; Coogan et al. 2016; Ring and Gerdes 2016; Roberts and Walker 2016; Nuriel et al. 2017; Roberts et al. 2017; Drost et al. 2018). MacDonald et al., (2019) used this technique to date calcite veins from ancient hydrothermal systems to show that closed-system bond reordering (Passey and Henkes 2012; Henkes et al. 2014; Stolper and Eiler 2015) did not affect determination of vein precipitation temperature from clumped isotopes.

In this contribution, we show that combining LA-ICP-MS U-Pb dating of calcite veins with stable isotope and trace element analyses can help to fingerprint fluid source when trace elements and fluid $\delta D$ & $\delta^{18}O$ cannot provide an unequivocal interpretation. We use a case study of volcanic-hosted veins in eastern Scotland, where this combination of proxies enables us to rule out magmatic fluids, indicating the fluid source of veins was meteoric water which had undergone significant water-rock interaction.

## GEOLOGICAL SETTING AND SAMPLE PETROGRAPHY

Calcite veins from Lunan Bay in Angus, Scotland formed the basis of this study (Fig. 1a-b). The study area is located within the northern part of the Midland Valley Terrane (e.g. Trewin 2002). The host rocks to the calcite veins are the Montrose Volcanic Formation (MVF), a group of mingled pahoehoe lavas, basaltic andesites, and volcanic-derived sediments deposited as part of the ~2000 m thick, sandstone dominated Arbuthnott-Garvock Group (e.g. Armstrong and Patterson 1970; Bluck 2000; Browne et al. 2002; Hole et al. 2013). These lavas are likely sourced from the northern flank of the Montrose Volcanic Centre, a north-east to south-west trending chain of volcanoes active for ~15 Ma. The MVF lavas are suggested to be coeval with the Rhynie lavas to the north, with a U-Pb andesite age of 411.5±1.3 Ma (Parry et al. 2011). This places the MVF within the late Lochkovian – early Pragian and at the boundary of the Arbuthnott and Garvock units (e.g. Armstrong and Patterson 1970; Bluck 2000; Browne et al. 2002; Hole et al. 2013).

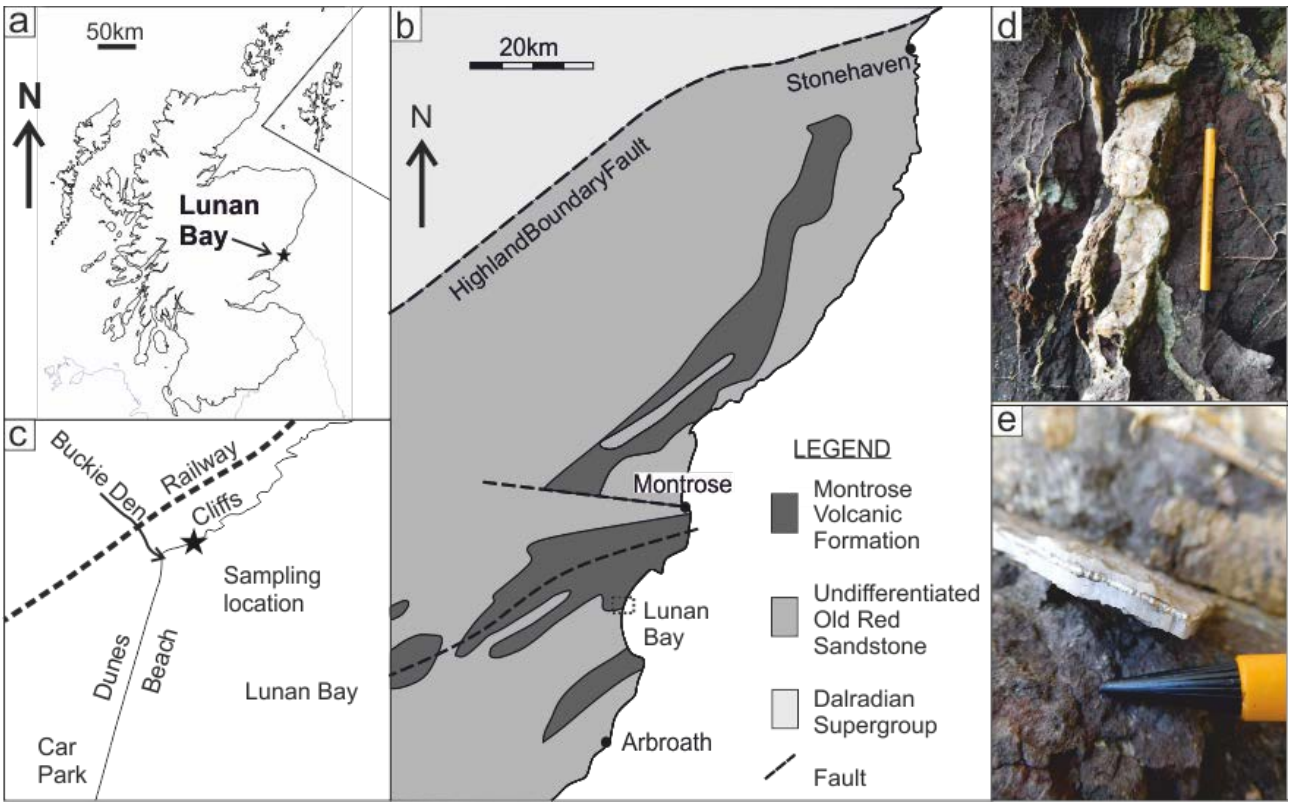


Figure 1: location and field photographs. (a) Location of Lunan Bay case study site within Scotland; (b) the distribution of the host Montrose Volcanic Formation in the region; (c) the detailed location of the samples; Field photographs of examples veins (d) JV17-1 and (e) JV17-11.

The MVF lavas are basaltic to basaltic andesite (5.2-8.6 wt.% MgO, 52.6-57.6 wt.% $SiO_2$) in composition, and samples from St. Cyrus region have been described as olivine-plagioclase phyric, with olivine commonly pseudomorphed to iddingsite (Thirlwall 1981; Thirlwall 1982; Thirlwall 1983). Sub-euhedral, tabular, microphenocrystic plagioclase feldspar (labradorite to low Ab andesine, An41-55) make up much of the matrix, along with abundant interstitial devitrified glass (Thirlwall 1982). Clinopyroxene is also present within some of the pahoehoe lava flows, predominantly in the form of augite (Hole et al. 2013). The lavas are also interbedded with locally sourced ephemeral playa-lake sediments, sandstones, and conglomerates, as well as air fall eruptions, creating complex sediment-lava interactions and abundant peperite formation (e.g. Hole et al. 2013). Within these mixing regions, secondary orthoclase is also present, as is sub-parallel flow alignment of feldspar laths and microphenocrysts (Thirlwall 1982; Thirlwall 1983).

Samples of MVF-hosted calcite veins were taken from the low cliffs just at the head of Lunan Bay at NO 69549 52488 (56°39’47.5”N, 02°29’54.1”W) (Fig. 1c). Images of vein petrography and relations to geochemical analysis are provided in Supplementary Figures S1-2. Most veins appear to be randomly oriented, with abundant stock work veining present; there is no clear field evidence of difference generations of veins. Five samples – JV17-1, -2, -9, -11 & -12 – were collected for analysis. The veins analysed in this study varied from >50 mm in width to less than 5 mm (Fig. 1d-e). Primary vein formation is along a singular opening (JV17-1, JV17-2, JV17-9), although some veins also occur as a bundle of connected sub parallel veins (JV17-12). Within these veins, multiple forms of calcite growth were recognized including bladed (JV17-1) and toothy (JV17-2, JV17-9) calcites along host rock contacts (Supp. Fig. S1), while euhedral, scalenohedral, and blocky crystals making up the bulk of most vein matrices (JV17-1, JV17-2, JV17-12) (Supp. Fig. S1). Crosscutting relationships and alteration are readily observed in JV17-1a, where a primarily syntaxial, bedrock growth phase is crosscut by a secondary, anhedral growth phase, and in JV17-11, where a stretched vein is crosscut by an iron rich vein. Multiple phases are also evidenced by bedrock fragments and remnant calcite crystal growth along these fragments that have been sealed within the vein during subsequent vein sealing (JV17-1, JV17-12) (Supp. Fig. S1).

JV17-11 contains the only formation of stretched beef-veining (appearing similar to beef tendons), progressing from stretched/bladed crystals with vein opening (Supp. Fig. S1), although other samples not included within this study were also observed to have significant beef veining. Minor veins are prevalent in many of the samples (JV171, JV17-2, JV17-9, JV17-11), predominantly sealed with fine, euhedral calcite crystals only a few mm in size. Accessory minerals (quartz and chlorite) are visible along the vein-bedrock contacts, while reddish sutures are visible during the final stage of vein formation/closure in JV17-1 and JV17-2, consisting primarily of iron oxides and other rare carbonate phases (Supp. Fig. S1). These suture-defined vugs are filled with predominantly cloudy, anhedral calcites. Despite the variations in texture, only JV17-11 exhibits antitaxial vein growth (Supp. Fig. S1).

Minor variations in CL can be seen within the larger individual euhedral-anhedral blocky crystals that make up the bulk of the vein matrix in JV17-1 and JV17-2 (Supp. Fig. S1). However, CL signatures are generally uniform across individual veins and amygdales despite textural variation, with primary excitation associated with calcite cleavage planes and extinction (Supp. Fig. S1).

## METHODS

Cathodoluminescence (CL) petrography was undertaken using a Lumin HC4-LM hot-cathode CL microscope at Saint Marys University. Plane-polarized and CL imagery was taken using an incorporated Olympus BXFM focusing unit and Kappa DX40C peltier cooled camera, controlled by the DX40C-285FW software package. The samples were analyzed under a vacuum, with an accelerating voltage of ~6 KV, a beam current of 0.25 mA, and a 1 s camera exposure time with a 6 db camera gain.

$\delta^{13}C$ and $\delta^{18}O$ measurements were made at either the Scottish Universities Environmental Research Centre (SUERC) or Memorial University Newfoundland's TERRA Stable Isotope Lab. At SUERC, 1 mg of powdered sample was digested in 100% phosphoric acid in a 25°C water bath prior to analysis in a VG OPTIMA mass spectrometer. A marble standard, as well as replicate analyses, were used to calibrate the results, with reproducibility in $\delta^{13}C$ of -9.2±0.1 ‰ and $\delta^{18}O$ of -15.0±0.1 ‰ (2σ) (Supp. Table S3). At Memorial, 0.2 mg of powdered sample was digested in 100% phosphoric acid in a 25°C water bath prior to analysis in a using a DeltaVPlus isotope ratio mass spectrometer (IRMS) equipped with a Thermo Electron GasBench II unit. NBS19, plus two internal standards, were used to calibrate the results, with NBS19 $\delta^{13}C$ of 2.0±0.1 ‰ and $\delta^{18}O$ of -2.2±0.1 ‰ (2σ), within error of accepted values (Friedman et al. 1982; Coplen et al. 2006) (Supp. Table S3).

δD values of fluid inclusions in calcite vein chips were measured by *in vacuo* decrepitation following the procedures outlined by Gleeson et al. (2008) at the Scottish Universities Environmental Research Centre (Supp. Table S4). Procedural reproducibility was tested with 3 in-house standards (Gleeson et al. 2008) and values were within 3 ‰ of long-term averages.

Carbonate clumped isotope ($\Delta_{47}$) measurements were carried out in the Isotopologue Paleosciences Laboratory at the University of Michigan, Ann Arbor. Samples were powdered using a dental drill. For $\Delta_{47}$ analysis, ~ 8 mg of sample powder was reacted in an automated preparation line previously described in Henkes et al., (2014). Carbonate powder was reacted under vacuum with 104% phosphoric acid at 90 °C for 10 min. Vapour-phase water generated during the reaction was separated from the produced $CO_2$ using liquid nitrogen swapped out an ethanol–liquid nitrogen mixture held at −85 °C. The water remained frozen while the $CO_2$ was passed through a Poropak Q chromatography trap held at −20 °C. The purified $CO_2$ was measured using a Nu Instruments Perspective isotope ratio mass spectrometer in dual inlet mode, with a measurement time of c. 2 h. All analyses were run as triplicates. Masses 44–49 were measured. Carrara marble, NBS19 and an in-house carbonate standard (102-GCAZ) were used to verify the results. Carrara Marble $\Delta_{47}$ averaged 0.417±0.022 ‰ (2σ, n=3), NBS19 $\Delta_{47}$ averaged 0.441±0.021 ‰ (2σ, n=10) and 102-GCAZ averaged 0.650±0.012 ‰ (2σ, n=14) during the analytical window. (Supp. Table S5).

All carbonate clumped isotope ($\Delta_{47}$) values in this study are presented on an absolute reference frame, also termed a 'carbon dioxide equilibrium scale' or CDES, which empirically corrects for instrumental nonlinearities and changes in the ionization environment during mass spectrometry (Dennis et al. 2011; Henkes et al. 2013). This reference frame was established by periodically analyzing aliquots of $CO_2$ that were isotopically equilibrated at 25 or 1000 $^{o}$C (Dennis

et al. 2011). Temperatures were calculated from $\Delta_{47}$ using the empirical "high temperature" $\Delta_{47}$ - temperature relationship from Bonifacie et al., (2017). Fluid $\delta^{18}O$ values were calculated using the equation of Friedman and O'Neil (1977).

Minor and trace element LA-ICP-MS analyses were undertaken at the Dalhousie Laboratory for Experimental High Pressure Geological Research using a New Wave Research frequency quintupled laser operating at 213 nm, coupled to a quadrupole mass spectrometer (PQ Excell or Thermo X-series) with He flushing. The analyses occurred as both linescans and spot analyses, with a 100µm spot size, ablated at 4-5 Hz with a 20% total energy. Concentrations of $^{43}Ca$, $^{55}Mn$, $^{57}Fe$, $^{85}Rb$, $^{86}Sr$, $^{87}Sr$, $^{89}Y$, $^{137}Ba$, $^{139}La$, $^{140}Ce$, $^{141}Pr$, $^{146}Nd$, $^{147}Sm$, $^{153}Eu$, $^{157}Gd$, $^{159}Tb$, $^{163}Dy$, $^{165}Ho$, $^{166}Er$, $^{169}Tm$, $^{172}Yb$, and $^{175}Lu$ were measured in blocks of sixteen analyses, with two NIST 610 bounding each block for a total of 20 analyses per run. Total run times were 140 s, with 20 s laser warm-up, 60 s ablation, and 60 s He-gas flushing time. However, due to calcite burn through, many analyses were between 20-30 s in order to prevent damage to the slide.

Data reduction was conducted off-line using Iolite software. Base levels were determined through $^{43}Ca$ peak analysis making sure to avoid anomalous intensities but also including washout periods. Analytical drift was addressed by running a linear regression through average $^{43}Ca$ intensities in the NIST SRM610 runs before and after unknown analyses; reproducibility in was better than 5% for all elements analysed in NIST SRM610. Average concentrations of all elements were within error of published values (Jochum et al. 2011) (Supp. Table S6). REE values were normalized to chondrite (McDonough and Sun 1995) using Microsoft Excel, following methods outlined in Rollinson (1993).

LA-ICP-MS U-Pb calcite dating was conducted at the Geochronology & Tracers Facility, British Geological Survey (Nottingham, UK) using a New Wave Research 193UC excimer laser ablation system, coupled to a Nu Instruments Attom single-collector sector-field ICP-MS following the methods outlined by Roberts and Walker (2016). Samples were pre-ablated with a 150 µm spot for 30 pulses. Full ablation conditions comprise a 100 µm spot for 30 seconds, at 10 Hz and a fluence of ca. 8 J/cm$^2$. A gas blank of ca. 60 seconds is measured at the beginning of each run. Normalisation uses NIST614 for $^{207}Pb/^{206}Pb$ and WC-1 for $^{206}Pb/^{238}U$, with data reduction and uncertainty propagation following Roberts et al., (2017) and the recommendations of Horstwood et al., (2016), and conducted using an in-house spreadsheet and the Nu Attolab Time Resolved Acquisition software. Spot analyses with low count rates (< 100 cps) or high uncertainties (>7.5% 1σ) are removed from age calculations. Age calculations and plotting were conducted using Isoplot 4.15 (Ludwig 2012). Duff Brown Tank limestone was analysed during the session as a validation material; an age of 63.5 ± 1.7 Ma (MSWD = 2.9) was obtained (Supp. Table S7), which overlaps the published age of 64.04 ± 0.67 Ma (Hill et al. 2016).

## RESULTS

The location of analyses of all types in the vein samples are shown in Supplementary Figures S1-2 and standard and sample geochemical data are given in Supplementary Tables S3-6. Across the 5 samples analysed, $\delta^{13}C$ ranged from -1.90 ‰ to -9.87 ‰ but with the majority between -3 and -4 ‰ (Table 1, Supp. Table S3). There was no clear correlation in $\delta^{13}C$ values and calcite crystal shape/vein texture or vein width at the point of analysis (Supp. Fig. S2). Vein calcite $\delta^{18}O$ (V-PDB) values ranged from -1.36 ‰ to -13.21 ‰ (Table 1, Supp. Table S3). Narrower veins tended to have more depleted $\delta^{18}O$ values, although this did not hold true for all samples, and $\delta^{18}O$ varied by several permil in single veins (up to ~10.5 ‰ between two adjacent analyses in vein JV17-1) (Table 1, Supp. Fig. S2). A δD value of -56.8 was obtained from fluid inclusions in calcite chips from JV17-1 (Table 1, Fig. 2a). Four clumped isotope temperatures were determined from three of the samples. The edge of the large vein in sample JV17-1 yielded a temperature of 111±42 °C while the centre of the same vein recorded 119±19 °C. A temperature of 161±27 °C was recorded from the centre of the large vein in JV17-2, and the set of sub-parallel linked veins in JV17-12 yielded a temperature of 166±46 °C (Table 1, Fig. 2b).

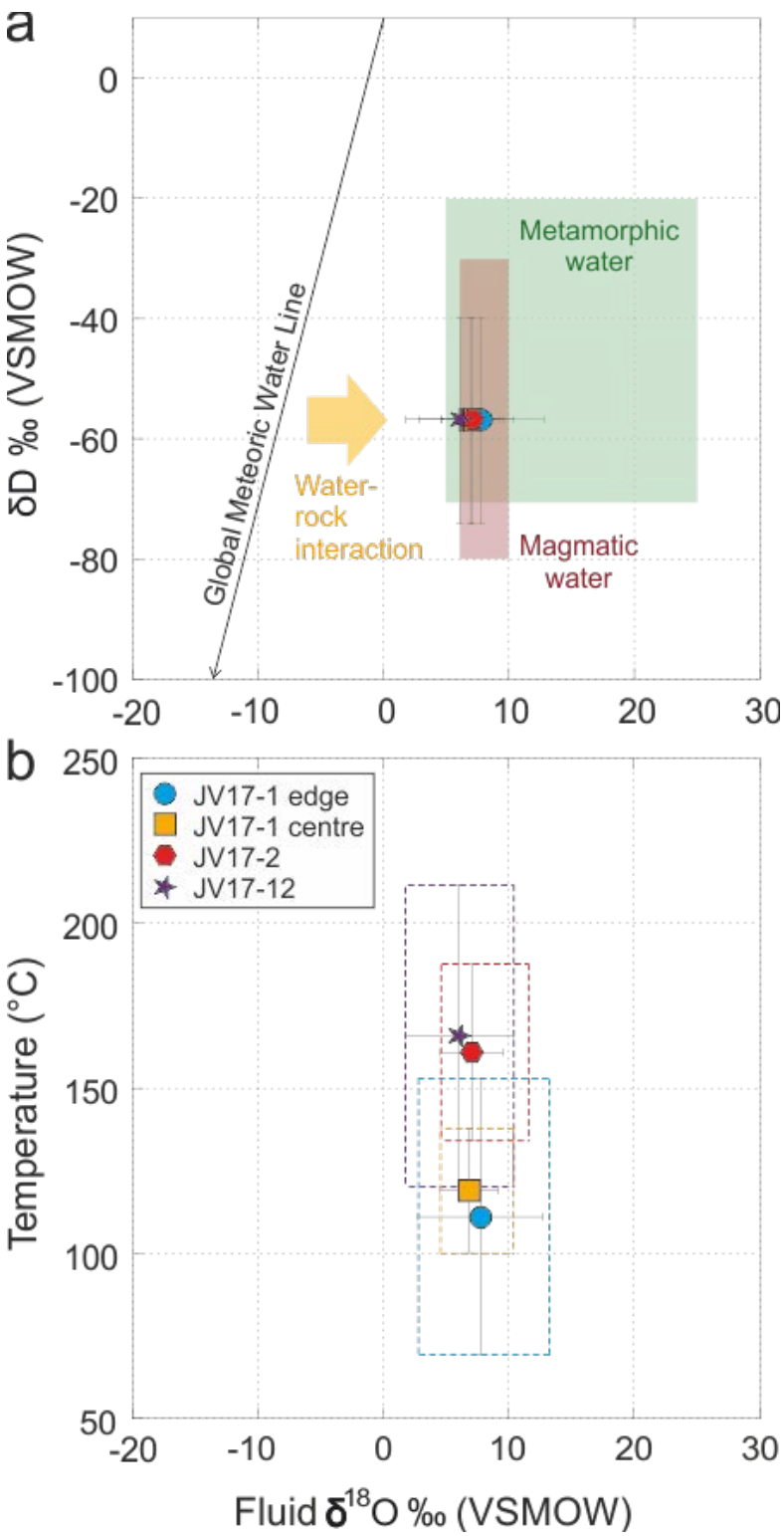


Figure 2: stable isotope data. a) Fluid δD and calculated fluid $\delta^{18}O$ values using Friedman and O'Neil (1977) equation with the temperature and calcite $\delta^{18}O$ from clumped isotope analyses; $\delta^{18}O$ error bars are 1 standard error propagated from the clumped isotope analysis while δD error bars represent the range of δD values obtained during the analysis; Global Meteoric Water Line from Craig (1961); range of typical isotopic composition of metamorphic water (e.g. Taylor, 1974; Hoefs, 2015) and magmatic water (e.g. Hoefs, 2015). b) temperature calculated using Bonifacie et al., (2017) $\Delta_{47}$-T calibration plotted against fluid $\delta^{18}O$; temperature error bars are 95% confidence level while fluid $\delta^{18}O$ error bars are the conventional 1 standard error; dashed boxes constrain the 95% confidence level temperature error and the maximum range of fluid $\delta^{18}O$ calculated from the clumped isotope temperatures and the range of calcite $\delta^{18}O$ measured in the different samples. Blue circle = JV17-1 edge; orange square = JV17-1 centre; red hexagon = JV17-2; purple star = JV17-12.

Fe concentrations were ~300-10000 ppm, with the majority <1000 ppm; Mn concentrations were ~700-12000 ppm. There was no clear correlation between Fe or Mn concentration and position across veins (i.e. edge to centre) and cathodoluminescence intensities were fairly uniform across all veins (Table 1, Supp. Fig. S2). Total Rare Earth Elements (ΣREE) values were ~1-1750 ppm (Table 1). In vein JV17-1, there was slight pattern of higher REE concentration at the vein edges than the core; however, this pattern was not present in the other wide vein (JV17-2) (Supp. Fig. S2). The other veins were too narrow for an assessment of REE concentration across the vein. All analyses had higher light REE concentrations than heavy REEs. A number of analyses had flat normalised LREE-MREE patterns; La/Gd ratios were usually lower than Gd/Lu ratios (Table 1). Ce anomalies were negligible, with Ce/Ce* values of 0.7-1.2, representing slight negative to slight positive anomalies (Table 1). Eu anomalies were also mainly negligible, with slight negative (0.7) to slight positive (1.2) values; a small number of analyses recorded more positive anomalies (1.5-2.0) (Table 1, Supp. Table S6).

One sample (JV17-2) yielded a calcite U-Pb age. The age of 318±30 Ma (MSWD = 1.4) was derived from regression of 89 spot analyses in that vein, with one analysis lying off the regression being rejected. This age includes propagation of the systematic uncertainties (Table 1, Fig. 3).

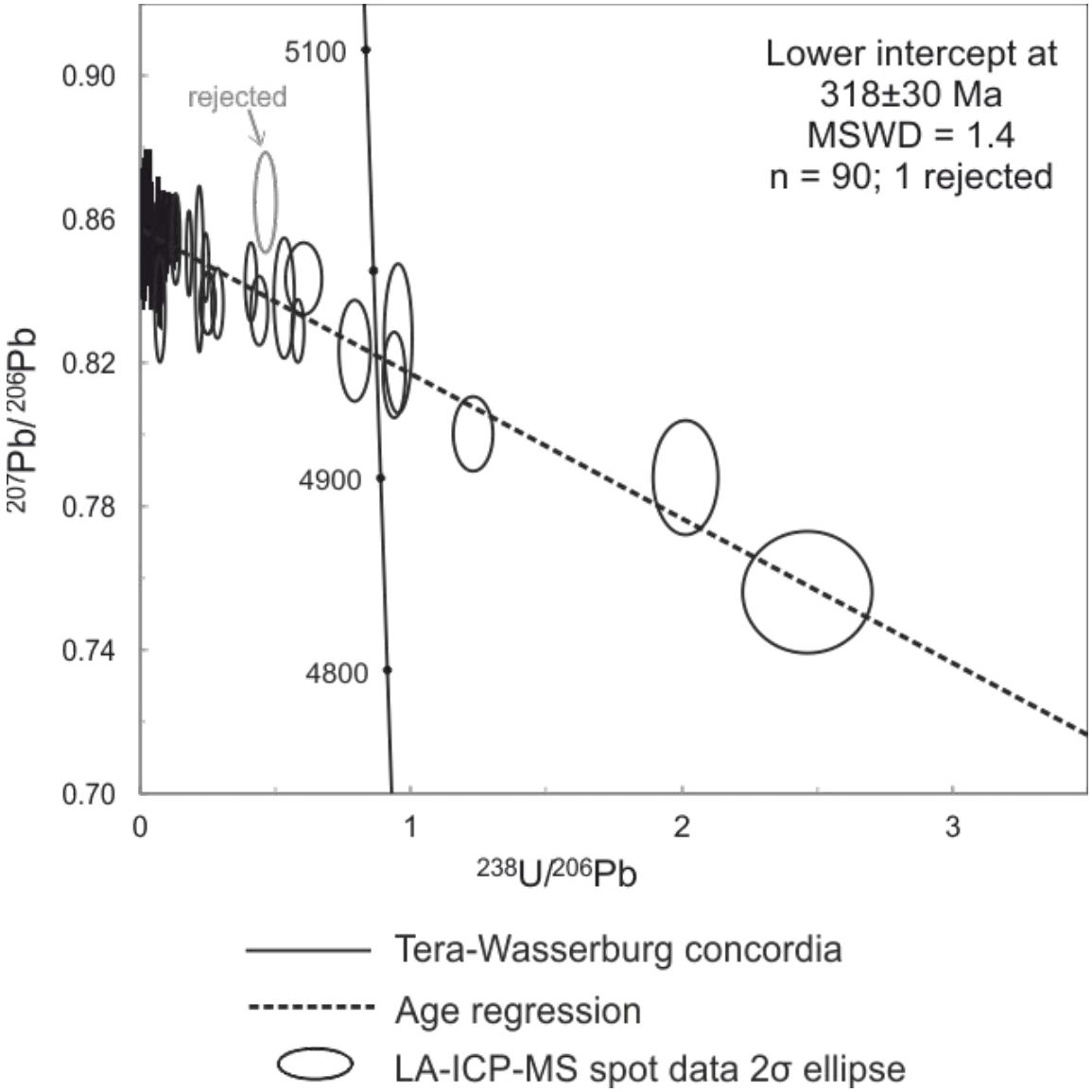


Figure 3: Tera-Wasserburg concordia plot showing age regression through LA-ICP-MS analytical spots (blue ellipses; rejected spot in grey); precipitation age defined as the lower intercept age of 318±30 Ma (2σ).

| Sample | Description | δD (VSMOW, ‰) | $\delta^{13}C$ (VPDB, ‰) | $\delta^{18}O_{cal}$ (VPDB, ‰) | $T_{\Delta47}$ (°C) | $\delta^{18}O_{fluid}$ (VSMOW, ‰) | Mn (ppm) | Fe (ppm) | ΣREE (ppm) | La/Gd | Gd/Lu | Ce/Ce* | Eu/Eu* | U-Pb Age (Ma) |
|---|---|---|---|---|---|---|---|---|---|---|---|---|---|---|
| JV17-1 | wide | -56.55 | -1.90 to -5.21 | -1.36 to -11.83 | *edge* 111±42 | 3.0 to 13.7 | 712-4230 | 373-846 | 4-1742 | 1.4-7.0 | 4.5-13.8 | 0.7-1.0 | 0.8-1.9 | - |
| | | | | | *centre* 119±19 | 4.9 to 10.6 | | | | | | | | |
| JV17-2 | wide | nd | -3.46 to -4.55 | -6.89 to -12.10 | 161±27 | 6.9 to 12.2 | 1996-6290 | 382-687 | 24-376 | 0.6-7.3 | 2.6-6.0 | 0.8-1.1 | 0.9-1.7 | 328±27 |
| JV17-9 | narrow | nd | -3.8 to -3.55 | -8.25 to -9.51 | - | - | 7070-9380 | 719-1320 | 248-769 | 8.7-10.7 | 13.1-19.6 | 0.7-0.9 | 0.7-0.8 | - |
| JV17-11 | narrow | nd | -5.64 to -9.87 | -10.77 to -12.89 | - | - | 3228-7001 | 447-5110 | 59-159 | 10.1-27.0 | 2.8-5.6 | 0.7-0.8 | 0.9-1.7 | - |
| JV17-12 | complex of connected sub-parallel narrow veins | nd | -3.04 to -3.35 | -12.18 to -13.21 | 166±46 | 6.1 to 7.1 | 1780-5390 | 509-670 | 53-280 | 4.1-11.0 | 1.9-10.7 | 0.7-0.9 | 0.9-2.0 | - |

Table 1: summary data table; 'nd' denotes not enough water was recovered from these samples to make a measurement.

## DISCUSSION

### *Stable Isotopes*

Calcite which has resided in the subsurface at high temperatures (ca. >100 °C) for a long period (ca. >100 Myr) is susceptible to solid-state bond reordering (Passey and Henkes 2012; Henkes et al. 2014; Shenton et al. 2015; Stolper and Eiler 2015). Passey and Henkes (2012) interpreted a two-stage bond reordering process of an initial phase of defect annealing followed by solid-state diffusion. Stolper and Eiler (2015) proposed different mechanisms: an initial rapid change of ~1-40 °C at ambient temperatures of ~75-120 °C sustained for ~100 Myr due to diffusion of isotopes through the crystal lattice; after a period of stability, a secondary stage of slow isotope exchange reactions between adjacent carbonate groups at >~150 °C sustained for >~100 Myr which may bring the clumped isotope temperatures to the ambient temperature.

Given that the calcite U-Pb dating indicates that the veins are much older than ca. 100 Myr, and clumped isotope thermometry yields temperatures of ca. 100 °C in all samples, thermal history reordering models (THRMs) were run to test for bond reordering (Supp. Table S8). The THRM approach developed by Shenton et al., (2015) involves modelling temporal evolution in $\Delta_{47}$ based on kinetic parameters (e.g., activation energy, $E_a$ and pre-exponential factor, $K_0$) derived from Arrhenius regressions of experimental data from Passey and Henkes (2012). THRMs require knowledge or assumptions about the temperature history of the analysed sample. This temperature history is divided into a series of time steps with a specified ambient temperature (converted back to $\Delta_{47}$) at each time step. The bond reordering reaction (reaction 13 in Passey and Henkes (2012)) is then used calculate the extent of clumped isotope reordering during each step. The 'new' $\Delta_{47}$ value at the end of each time step is treated as the 'initial' $\Delta_{47}$ value for the next step and the model is run iteratively from the time of initial calcite precipitation to the present day (Shenton et al. 2015). Additionally, calcite of different origin (e.g. brachiopods vs spar calcite vs optical calcite) were found to have different reordering kinetics (activation energy and pre-exponential factor) during laboratory experiments (Passey and Henkes 2012; Henkes et al. 2014).

In addition to the activation energy and pre-exponential factor, the assumed initial precipitation temperature and age of precipitation are input to run the model. For sedimentary or biogenic calcite, an assumed surface temperature of ca. 25 °C (or a more accurate one based on species in biogenic calcites) is used (Henkes et al. 2013; Henkes et al. 2014). For calcite veins this is challenging as one cannot assume an initial precipitation temperature. We assumed that the temperature reconstructed from clumped isotope analysis was the initial precipitation temperature and forward modelled using an ambient thermal history to determine if bond reordering had occurred.

THRMs were run for all samples using the burial history for the local area constructed from vitrinite reflectance data and an assumed geotherm of 30 °C/km (Marshall et al. 1994), along with the calcite precipitation ages derived in this study from LA-ICP-MS calcite U-Pb dating. Kinetic parameters for both optical and spar (labile and refractory) calcite from Passey and Henkes (2012) were used but the choice of kinetic parameters did not affect the model output. This is because the THRMs indicate that negligible (much less than analytical error) bond reordering took place in any of these samples (Fig. 4).

Clumped isotope temperatures from the centre and edge of the large vein in sample JV17-1 are within error, suggesting that temperature remained relatively constant during calcite precipitation. However, the temperatures from JV17-1 are ~50 °C lower than in JV17-2 and JV17-12. The origin of this difference is unclear but may reflect an age difference – JV17-1 may be younger than JV17-2 and JV17-12 and records a cooling of the vein-forming fluid. Unfortunately, it was not possible to obtain an age from JV17-1 and so this cannot be proven. Calcite $\delta^{18}O$ (V-PDB)

values varied by several permil within veins, suggesting that as well as some minor temperature variation within veins, slight variation in source fluid $\delta^{18}O$ and/or interaction with oxygen from the wall rocks of the veins resulted in variability in calcite $\delta^{18}O$. As the THRMs have shown that the clumped isotope temperatures do indeed represent the calcite precipitation temperature, the $\delta^{18}O$ of the parent fluids can be reconstructed.

In sample JV17-1, calculated fluid $\delta^{18}O$ (V-SMOW) values ranges from 3 to 14 ‰, but with the majority in the 7-9 ‰ range. Similarly for JV17-2, values are ~7-12 ‰, with most 7-9 ‰. In sample JV17-12, values are ~6-7 ‰ (Table 1, Fig. 2). Values such as these represent fluids isotopically enriched relative to VSMOW and are typical of metamorphic waters, magmatic waters, or meteoric/marine waters which have undergone significant fluid-rock interaction (e.g. Sharp 2007). Barker et al., (2009) suggested that homogeneity of calcite $\delta^{18}O$ across veins may indicate the progressive reaction of fluids with host rock, with sufficient reaction occurring along discrete fluid flow pathways to fully equilibrate the fluids for these isotope systems. Samples JV17-9, JV17-11 and JV17-12 (narrow veins) display this homogeneity (<~2 ‰ variation), as does large vein JV17-2 apart from a single analysis at the very edge of the vein which is ~3 ‰ less depleted than the rest of the analyses from that vein (Supp. Fig. S2). Sample JV17-1, however, displays a wide range in calcite $\delta^{18}O$. Additionally, $\delta^{13}C$ values are all negative which suggest oxidised fluids (Barker et al. 2006) which is more likely to be a surface water but is not conclusive. The δD values are also inconclusive and could represent metamorphic, magmatic or meteoric waters. Even when taking δD and $\delta^{18}O$ together, the samples fall within the field of typical magmatic and metamorphic waters or could represent meteoric water which has undergone significant water-rock interaction (e.g. Taylor 1974; Rollinson 1993; Sharp 2007; Hoefs 2015) (Fig. 2b). Stable isotopes and reconstructed fluid $\delta^{18}O$ alone can therefore not distinguish fluid sources.

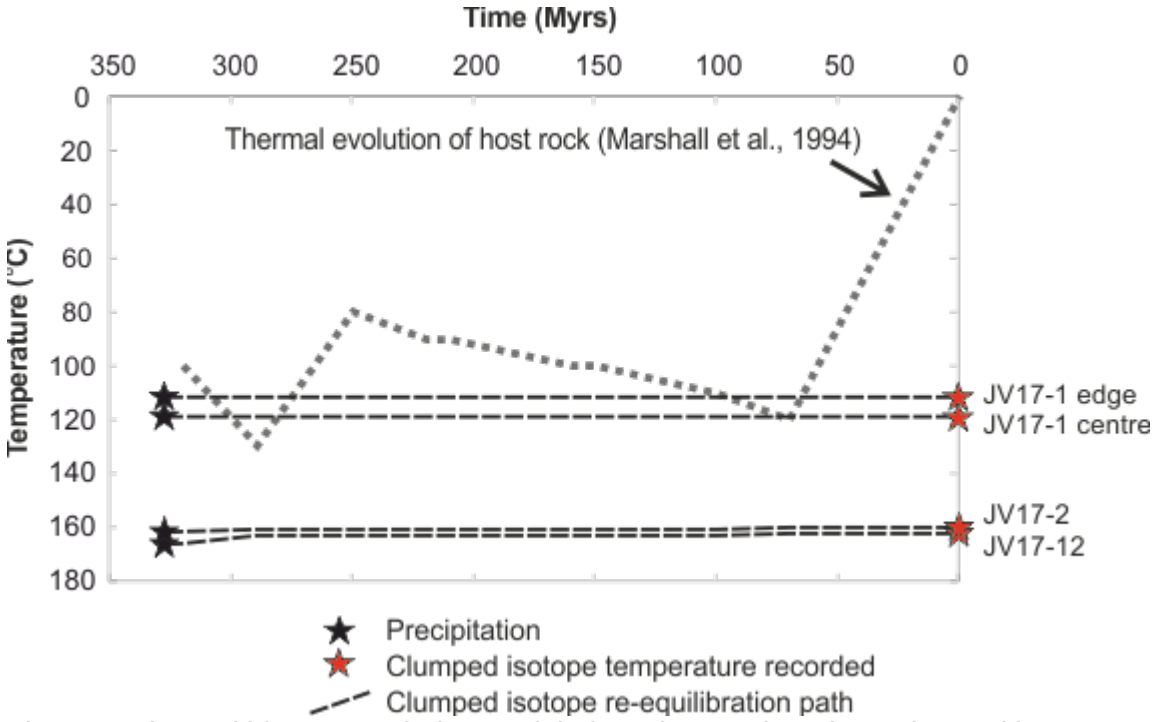


Figure 4: Thermal history reordering models for vein samples where clumped isotope temperatures were obtained showing the modelled evolution of clumped isotope temperature (calculated using the equations in Passey et al., (2012) and the approach of Shenton et al., (2015)) and ambient temperature after vein precipitation (from Marshall et al., (1994)).

*Trace Elements*

All REEs are incompatible in basalt/andesite (the host rocks to this study) (e.g. Rollinson 1993) and so are easily scavenged by fluids. Calcite fractionates LREE over HREE during precipitation, leading to the negatively-sloping normalised REE patterns (e.g. Bau and Möller 1992; Denniston et al. 1997; Morad et al. 2010) as indicated by positive La/Gd and Gd/Lu ratios (Table 1). REE concentrations in the calcite veins in this study are higher than in typical freshwater/seawater (e.g. Rollinson 1993; Morad et al. 2010), suggesting metamorphic/magmatic fluids or

freshwater/seawater which has undergone significant water-rock interaction. This agrees with the interpretation of the reconstructed fluid $\delta^{18}O$ values but still does not fingerprint a particular source fluid.

Conceptually, in a wider vein, e.g. JV17-1, if there was a lot of fluid-rock interaction then minor and trace element concentrations would be expected to be higher at the vein edge than the centre (assuming growth out from the vein edge as the petrographic analysis suggests); initial reaction of the fluid with the fracture walls would scavenge trace elements (e.g. incompatible REEs) and incorporate these in precipitated calcite. As the vein infilled, initially-precipitated calcite would 'armour' the wall rock from the fluid and so later calcite, precipitated in the centre of the vein, would have lower REE concentrations. There is a suggestion of this in total REE in JV17-1 but not clearly (Supp. Fig. S2); however, such a pattern does not occur in veins JV17-2 or JV17-12 (Supp. Fig. S2). This pattern of higher trace element concentration at vein edges is also not shown clearly by Fe or Mn in any of the analysed veins (Supp. Fig. S2).

Similarly, conceptually, in narrow veins all the calcite might be expected to have higher REE concentrations given the lower calcite-wall rock ratio. This is not borne out by the total REEs but high La/Gd values – signifying strong fractionation of LREEs into the calcite – are found in narrow veins JV17-9 and JV17-11 (Table 1). JV17-9 in particular also shows the highest concentrations of Mn, again indicating significant fluid-rock interaction (Table 1).

The veins generally showed no strongly positive Eu anomalies which suggests little interaction with Ca-rich bedrock, as Eu substitutes for Ca, predominantly in plagioclase (Barker et al 2006). The MVF is high in Ca (in clinopyroxene and plagioclase) and so extensive water-rock interaction would be expected to lead to positive Eu anomalies. This is generally not seen although some spots do have strongly positive Eu anomalies (up to 2.0); these do not appear to clearly correlate with position in the vein in relation to the wall rock or calcite petrography (Supp. Fig. S2). The Eu anomaly is therefore inconclusive regarding the origin of the fluid.

The Ce anomaly can be used as a redox proxy for fluids in veins, where a negative Ce anomaly indicates oxidising conditions (e.g. Göb et al. 2013). No strongly negative (or positive) Ce anomalies were found in the veins in this study, indicating the fluid was not highly oxidised at the time of calcite precipitation. While well-oxidised surface waters have negative Ce anomalies, fluids which originate from the subsurface (magmatic/metamorphic fluids) or surface waters which have resided in the crust for some time and undergone water-rock interaction show no Ce anomaly (e.g. Göb et al. 2013). The Ce anomaly is therefore in agreement with the stable isotope data, in that the fluid from which the veins precipitated from was either a magmatic/metamorphic fluid, or a meteoric/marine water which had undergone significant water-rock interaction. No correlation was found between calcite crystal microstructure and stable isotopes/trace elements (Supp. Fig. S2). This lack of correlation, and inability to fingerprint the source fluid, was also encountered by Maskenskaya et al., (2014) in a previous study.

*Calcite Geochronology*

Based on stable isotopes and trace elements, it has not been possible to distinguish the fluid source which formed the calcite veins between either a deep isotopically-enriched fluid (magmatic or metamorphic water) or a surface water which has undergone significant water-rock interaction. Simply based on the local geology, metamorphic waters can likely be ruled out as the fluid source as the nearest exposed metamorphic rocks are ~25 km away beyond the Highland Boundary Fault and the age of metamorphism (~470 Ma, Viete et al. 2013) long predates the formation of the Devonian MVF host rocks to the calcite veins.

Magmatic waters remain a viable fluid source as the host rocks are volcanic, and sporadic volcanic activity occurred through time in the Midland Valley Terrane (Cameron and Stephenson 1985). Determining whether magmatic waters are a likely fluid source requires the age of calcite precipitation in the veins to be known, so that that age can then be compared to ages of volcanic/magmatic activity in the local area. If vein calcite precipitation occurred very soon after the formation of the MVF from residual waters from the volcanic activity, then the calcite should yield an age within error of the MVF crystallisation age. Given that the MVF is correlated with the Rhynie Chert dated at 411.5±1.3 Ma (Parry et al. 2011) and the calcite precipitation age is 318±30 Ma, this shows that the calcite did not form from a magmatic fluid associated with the formation of the host MVF. There is some Lower Carboniferous (potentially within uncertainty of the age from the Lunan Bay calcite veins) volcanic activity in the Midland Valley Terrane, but the nearest is located several

tens of kilometres to the south around St Andrews (Cameron and Stephenson 1985), and so it is unlikely that magmatic fluids associated with this volcanic activity were the source fluids for the calcite veins.

*Importance of Calcite Geochronology in Fingerprinting Vein Fluid Sources*

LA-ICP-MS U-Pb calcite dating has enabled us to rule out magmatic fluids as the source for calcite veins hosted in basaltic andesites when stable isotopes and trace elements were unable to do so. For the Lunan Bay calcite veins, the fluid source must be a surface water which has undergone considerable fluid-rock interaction, leading to the enriched fluid $\delta^{18}O$ reconstructed from stable isotope analysis and clumped isotope thermometry. Palaeogeographic reconstructions indicate that the area was coastal terrestrial lowland for much of the Carboniferous (Cope et al. 1992), and we interpret that this surface water was likely meteoric water, rather than seawater/brine.

This case study from Lunan Bay highlights, along with previous studies from other locations (e.g. Maskenskaya et al. 2014), the difficulty in fingerprinting fluid source from stable isotopes and/or trace elements. In this study, LA-ICP-MS U-Pb calcite geochronology helped eliminate potential fluid sources, enabling determination of the most likely fluid source for the analysed calcite veins. It is an additional proxy that should be used alongside stable isotopes and trace elements in studies where the fluid source of veins, or indeed any other geological feature where the parent fluid may have resided in the crust for a period of time such as fault precipitates (e.g. Roberts and Walker 2016; Parrish et al. 2018) or cements (e.g. Mangenot et al. 2018b; Pagel et al. 2018).

## CONCLUSIONS

In this contribution we have shown that combining LA-ICP-MS U-Pb calcite dating with stable isotopes (including clumped isotope palaeothermometry) and trace element analysis increases the likelihood of determining the fluid source of veins. Calcite veins hosted in the Devonian Montrose Volcanic Formation at Lunan Bay in the Midland Valley Terrane of Central Scotland were used as a case study. $\delta D$ values of fluid inclusions in the calcite, and parent fluid $\delta^{18}O$ values reconstructed from clumped isotope palaeothermometry, gave values which could represent a range of fluid sources: metamorphic or magmatic fluids, or surface waters which had undergone much fluid-rock interaction. Trace elements showed no distinctive patterns and shed no further light on fluid source. LA-ICP-MS U-Pb dating determined the vein calcite precipitation age – 318±30 Ma – which rules out metamorphic or magmatic fluid sources as no metamorphic or magmatic activity was occurring in the area at this time. The vein fluid source was therefore a surface water (meteoric based on paleogeographic reconstruction) which had undergone significant water-rock interaction. This study highlights the importance of combining the recently developed LA-ICP-MS U-Pb calcite geochronometer with stable isotopes and trace elements to help determine fluid sources of veins, and indeed any geological feature where calcite precipitated from a fluid which may have resided in the crust for a period of time (e.g. fault precipitates or cements).

## ACKNOWLEDGEMENTS

Dr James Brenan and Dan MacDonald, Dalhousie University, are thanked for assistance using LA-ICP-MS; Alison McDonald is helped for assistance with the stable isotope analysis at SUERC.

## FUNDING

JV received funding from Dalhousie University's Shell Educational Learning Fund (SELF) and the Society of Economic Geologists Canada Foundation (SEGCF) undergraduate research fund. Fieldwork was part-funded by Research Incentive Grant 70316 from the Carnegie Trust for the Universities of Scotland to JMM and JF.

## REFERENCES

Armstrong M & Patterson IB (1970) The Lower Old Red Sandstone of the Strathmore Region. In, Report of the Institute of Geological Sciences, **70/12**.

Barker CE & Goldstein RH (1990) Fluid-inclusion technique for determining maximum temperature in calcite and its comparison to the vitrinite reflectance geothermometer. *Geology*, **18**,1003-1006.

Barker SLL, Bennett VC, Cox SF, Norman MD & Gagan MK (2009) Sm–Nd, Sr, C and O isotope systematics in hydrothermal calcite–fluorite veins: Implications for fluid–rock reaction and geochronology. *Chemical Geology*, **268**,58-66.

Barker SLL & Cox SF (2011) Oscillatory zoning and trace element incorporation in hydrothermal minerals: insights from calcite growth experiments. *Geofluids*, **11**,48-56.

Barker SLL, Cox SF, Eggins SM & Gagan MK (2006) Microchemical evidence for episodic growth of antitaxial veins during fracture-controlled fluid flow. *Earth and Planetary Science Letters*, **250**,331-344.

Bau M & Möller P (1992) Rare earth element fractionation in metamorphogenic hydrothermal calcite, magnesite and siderite. *Mineralogy and Petrology*, **45**,231-246.

Bergman SC, Huntington KW & Crider JG (2013) Tracing paleofluid sources using clumped isotope thermometry of diagenetic cements along the Moab Fault, Utah. *American Journal of Science*, **313**,490-515.

Bluck BJ (2000) Old Red Sandstone basins and alluvial systems of Midland Scotland. In: *New Perspectives on the Old Red Sandstone* (eds Friend PF & Williams BPJ) London, The Geological Society, **180**, 417-437.

Bonifacie M, Calmels D, Eiler JM, Horita J, Chaduteau C, Vasconcelos C, Agrinier P, Katz A, Passey BH, Ferry JM & Bourrand J-J (2017) Calibration of the dolomite clumped isotope thermometer from 25 to 350 °C, and implications for a universal calibration for all (Ca, Mg, Fe)CO3 carbonates. *Geochimica et Cosmochimica Acta*, **200**,255-279.

Browne MAE, Smith RA & Aitken AM (2002) Stratigraphical framework for the Devonian (Old Red Sandstone) rocks of Scotland south of a line from Fort William to Aberdeen. In, British Geological Survey.

Cameron IB & Stephenson D (1985) *British Regional Geology: The Midland Valley of Scotland*, 3rd edn. London, HMSO.

Coogan LA, Parrish RR & Roberts NMW (2016) Early hydrothermal carbon uptake by the upper oceanic crust: Insight from in situ U-Pb dating. *Geology*, **44**,147-150.

Cope JCW, Ingham JK & Rawson PF (1992) *Atlas of Palaeogeography and Lithofacies*. London, Geological Society.

Coplen TB, Brand WA, Gehre M, Gröning M, Meijer HAJ, Toman B & Verkouteren RM (2006) New Guidelines for δ13C Measurements. *Analytical Chemistry*, **78**,2439-2441.

Craig H (1961) Isotopic Variations in Meteoric Waters. *Science*, **133**,1702-1703.

Dennis KJ, Affek HP, Passey BH, Schrag DP & Eiler JM (2011) Defining an absolute reference frame for 'clumped' isotope studies of $CO_2$. *Geochimica et Cosmochimica Acta*, **75**,7117-7131.

Denniston RF, Shearer CK, Layne GD & Vaniman DT (1997) SIMS analyses of minor and trace element distributions in fracture calcite from Yucca Mountain, Nevada, USA. *Geochimica et Cosmochimica Acta*, **61**,1803-1818.

Drost K, Chew D, Petrus JA, Scholze F, Woodhead JD, Schneider JW & Harper DAT (2018) An Image Mapping Approach to U-Pb LA-ICP-MS Carbonate Dating and Applications to Direct Dating of Carbonate Sedimentation. *Geochemistry, Geophysics, Geosystems*, **19**,4631-4648.

Eiler JM (2007) "Clumped-isotope" geochemistry—The study of naturally-occurring, multiply-substituted isotopologues. *Earth and Planetary Science Letters*, **262**,309-327.

Epstein S, Buchsbaum R, Lowenstam H & Urey H (1951) Carbonate-Water Isotopic Temperature Scale. *Bulletin Of The Geological Society Of America*, **62**,417-426.

Friedman I & O'Neil J (1977) Compilation of stable isotope fractionation factors of geochemical interest. In: *US Geol Surv Prof Paper*, **440-KK**.

Friedman I, O'Neil J & Cebula G (1982) Two New Carbonate Stable-Isotope Standards. *Geostandards Newsletter*, **6**,11-12.

Gleeson SA, Roberts S, Fallick AE & Boyce AJ (2008) Micro-Fourier Transform Infrared (FT-IR) and δD value investigation of hydrothermal vein quartz: Interpretation of fluid inclusion δD values in hydrothermal systems. *Geochimica et Cosmochimica Acta*, **72**,4595-4606.

Göb S, Loges A, Nolde N, Bau M, Jacob DE & Markl G (2013) Major and trace element compositions (including REE) of mineral, thermal, mine and surface waters in SW Germany and implications for water–rock interaction. *Applied Geochemistry*, **33**,127-152.

Henkes GA, Passey BH, Grossman EL, Shenton BJ, Perez-Huerta A & Yancey TE (2014) Temperature limits for preservation of primary calcite clumped isotope paleotemperatures. *Geochimica et Cosmochimica Acta*, **139**,362-382.

Henkes GA, Passey BH, Wanamaker AD, Grossman EL, Ambrose WG & Carroll ML (2013) Carbonate clumped isotope compositions of modern marine mollusk and brachiopod shells. *Geochimica et Cosmochimica Acta*, **106**,307-325.

Hill CA, Polyak VJ, Asmerom Y & P. Provencio P (2016) Constraints on a Late Cretaceous uplift, denudation, and incision of the Grand Canyon region, southwestern Colorado Plateau, USA, from U-Pb dating of lacustrine limestone. *Tectonics*, **35**,896-906.

Hodson KR, Crider JG & Huntington KW (2016) Temperature and composition of carbonate cements record early structural control on cementation in a nascent deformation band fault zone: Moab Fault, Utah, USA. *Tectonophysics*, **690**,240-252.

Hoefs J (2015) *Stable Isotope Geochemistry*, 7th edn, Springer.

Hole M, Jolley D, Hartley A, Leleu S, John N & Ball M (2013) Lava–sediment interactions in an Old Red Sandstone basin, NE Scotland. *Journal of the Geological Society*, **170**,641-655.

Horstwood MSA, Košler J, Gehrels G, Jackson SE, McLean NM, Paton C, Pearson NJ, Sircombe K, Sylvester P, Vermeesch P, Bowring JF, Condon DJ & Schoene B (2016) Community-Derived Standards for LA-ICP-MS U-(Th-)Pb Geochronology – Uncertainty Propagation, Age Interpretation and Data Reporting. *Geostandards and Geoanalytical Research*, **40**,311-332.

Jochum KP, Weis U, Stoll B, Kuzmin D, Yang Q, Raczek I, Jacob DE, Stracke A, Birbaum K, Frick DA, Günther D & Enzweiler J (2011) Determination of Reference Values for NIST SRM 610–617 Glasses Following ISO Guidelines. *Geostandards and Geoanalytical Research*, **35**,397-429.

Kalliomäki H, Wagner T, Fusswinkel T & Schultze D (2019) Textural evolution and trace element chemistry of hydrothermal calcites from Archean gold deposits in the Hattu schist belt, eastern Finland: Indicators of the ore-forming environment. *Ore Geology Reviews*, **112**,103006.

Li Q, Parrish RR, Horstwood MSA & McArthur JM (2014) U-Pb dating of cements in Mesozoic ammonites. *Chemical Geology*, **376**,76-83.

Lu Y-C, Song S-R, Taguchi S, Wang P-L, Yeh E-C, Lin Y-J, MacDonald J & John CM (2018) Evolution of hot fluids in the Chingshui geothermal field inferred from crystal morphology and geochemical vein data. *Geothermics*, **74**,305-318.

Lu Y-C, Song S-R, Wang P-L, Wu C-C, Mii H-S, MacDonald J, Shen C-C & John CM (2017) Magmatic-like fluid source of the Chingshui geothermal field, NE Taiwan evidenced by carbonate clumped-isotope paleothermometry. *Journal of Asian Earth Sciences*, **149**,124-133.

Ludwig KR (2012) User's Manual for Isoplot 3.75-4.15. In, Berkeley Geochronology Center.

MacDonald JM, Faithfull JW, Roberts NMW, Davies AJ, Holdsworth CM, Newton M, Williamson S, Boyce A & John CM (2019) Clumped-isotope palaeothermometry and LA-ICP-MS U–Pb dating of lava-pile hydrothermal calcite veins. *Contributions to Mineralogy and Petrology*, **174**,63.

Mangenot X, Gasparrini M, Gerdes A, Bonifacie M & Rouchon V (2018a) An emerging thermochronometer for carbonate-bearing rocks: Delta(47)/(U-Pb). *Geology*, **46**,1067-1070.

Mangenot X, Gasparrini M, Rouchon V & Bonifacie M (2018b) Basin-scale thermal and fluid flow histories revealed by carbonate clumped isotopes ((47)) - Middle Jurassic carbonates of the Paris Basin depocentre. *Sedimentology*, **65**,123-150.

Marshall JEA, Haughton PDW & Hillier SJ (1994) Vitrinite reflectivity and the structure and burial history of the Old Red Sandstone of the Midland Valley of Scotland. *Journal of the Geological Society*, **151**,425-438.

Maskenskaya OM, Drake H, Broman C, Hogmalm JK, Czuppon G & Åström ME (2014) Source and character of syntaxial hydrothermal calcite veins in Paleoproterozoic crystalline rocks revealed by fine‐scale investigations. *Geofluids*, **14**,495-511.

McDonough WF & Sun Ss (1995) The composition of the Earth. *Chemical Geology*, **120**,223-253.

Menzies CD, Teagle DAH, Craw D, Cox SC, Boyce AJ, Barrie CD & Roberts S (2014) Incursion of meteoric waters into the ductile regime in an active orogen. *Earth and Planetary Science Letters*, **399**,1-13.

673 Morad S, Al-Aasm IS, Sirat M & Sattar MM (2010) Vein calcite in cretaceous carbonate reservoirs
674 of Abu Dhabi: Record of origin of fluids and diagenetic conditions. *Journal of Geochemical*
675 *Exploration*, **106**,156-170.
676 Nuriel P, Weinberger R, Kylander-Clark ARC, Hacker BR & Craddock JP (2017) The onset of the
677 Dead Sea transform based on calcite age-strain analyses. *Geology*, **45**,587-590.
678 Pagel M, Bonifacie M, Schneider DA, Gautheron C, Brigaud B, Calmels D, Cros A, Saint-Bezar B,
679 Landrein P, Sutcliffe C, Davis D & Chaduteau C (2018) Improving paleohydrological and
680 diagenetic reconstructions in calcite veins and breccia of a sedimentary basin by combining
681 Delta(47) temperature, delta O-18(water) and U-Pb age. *Chemical Geology*, **481**,1-17.
682 Parrish RR, Parrish CM & Lasalle S (2018) Vein calcite dating reveals Pyrenean orogen as cause
683 of Paleogene deformation in southern England. *Journal of the Geological Society*.
684 Parry SF, Noble SR, Crowley QG & Wellman CH (2011) A high-precision U–Pb age constraint on
685 the Rhynie Chert Konservat-Lagerstätte: time scale and other implications. *Journal of the*
686 *Geological Society*, **168**,863-872.
687 Passey BH & Henkes GA (2012) Carbonate clumped isotope bond reordering and
688 geospeedometry. *Earth and Planetary Science Letters*, **351-352**,223-236.
689 Ring U & Gerdes A (2016) Kinematics of the Alpenrhein-Bodensee graben system in the Central
690 Alps: Oligocene/Miocene transtension due to formation of the Western Alps arc. *Tectonics*,
691 **35**,1367-1391.
692 Roberts NMW, Rasbury ET, Parrish RR, Smith CJ, Horstwood MSA & Condon DJ (2017) A calcite
693 reference material for LA-ICP-MS U-Pb geochronology. *Geochemistry Geophysics*
694 *Geosystems*, **18**,2807-2814.
695 Roberts NMW & Walker RJ (2016) U-Pb geochronology of calcite-mineralized faults: Absolute
696 timing of rift-related fault events on the northeast Atlantic margin. *Geology*, **44**,531-534.
697 Rollinson H (1993) *Using Geochemical Data: Evaluation, Presentation, Interpretation*. Harlow,
698 Pearson Prentice Hall.
699 Schauble EA, Ghosh P & Eiler JM (2006) Preferential formation of 13C–18O bonds in carbonate
700 minerals, estimated using first-principles lattice dynamics. *Geochimica et Cosmochimica*
701 *Acta*, **70**,2510-2529.
702 Sharp Z (2007) *Principles of Stable Isotope Geochemistry*. New Jersey, Pearson Prentice Hall.
703 Shenton BJ, Grossman EL, Passey BH, Henkes GA, Becker TP, Laya JC, Perez-Huerta A, Becker
704 SP & Lawson M (2015) Clumped isotope thermometry in deeply buried sedimentary
705 carbonates: The effects of bond reordering and recrystallisation. *GSA Bulletin*, **127**.
706 Simmons SF & Christenson BW (1994) Origins of calcite in a boiling geothermal system. *American*
707 *Journal of Science*, **294**,361-400.
708 Stolper DA & Eiler JM (2015) The kinetics of solid-state isotope-exchange reactions for clumped
709 isotopes: A study of inorganic calcites and apatites from natural and experimental samples.
710 *American Journal of Science*, **315**,363-411.
711 Sturrock CP, Catlos EJ, Miller NR, Akgun A, Fall A, Gabitov RI, Yilmaz IO, Larson T & Black KN
712 (2017) Fluids along the North Anatolian Fault, Niksar basin, north central Turkey: Insight
713 from stable isotopic and geochemical analysis of calcite veins. *Journal of Structural*
714 *Geology*, **101**,58-79.
715 Taylor HP (1974) The Application of Oxygen and Hydrogen Isotope Studies to Problems of
716 Hydrothermal Alteration and Ore Deposition. *Economic Geology*, **69**,843-883.
717 Thirlwall MF (1981) Implications for Caledonian plate tectonic models of chemical data from
718 volcanic rocks of the British Old Red Sandstone. *Journal of the Geological Society*,
719 **138**,123-138.
720 Thirlwall MF (1982) Systematic variation in chemistry and Nd-Sr isotopes across a Caledonian
721 calc-alkaline volcanic arc: implications for source materials. *Earth and Planetary Science*
722 *Letters*, **58**,27-50.
723 Thirlwall MF (1983) Isotope geochemistry and origin of calc-alkaline lavas from a caledonian
724 continental margin volcanic arc. *Journal of Volcanology and Geothermal Research*, **18**,589-
725 631.
726 Trewin NH (2002) The Building Blocks, The Terranes of Scotland. In: *The Geology of Scotland*,
727 Geological Society of London, 0.

Uysal IT, Feng Y-x, Zhao J-x, Bolhar R, Işik V, Baublys KA, Yago A & Golding SD (2011) Seismic cycles recorded in late Quaternary calcite veins: Geochronological, geochemical and microstructural evidence. *Earth and Planetary Science Letters*, **303**,84-96.

Viete DR, Oliver GJH, Fraser GL, Forster MA & Lister GS (2013) Timing and heat sources for the Barrovian metamorphism, Scotland. *Lithos*, **177**,148-163.

Wagner T, Boyce AJ & Erzinger J (2010) Fluid-rock interaction during formation of metamorphic quartz veins: A REE and stable isotope study from the Rhenish Massif, Germany. *American Journal of Science*, **310**,645-682.